Hydrolysis Mechanisms for the Organopalladium Complex [Pd(CNN)P(OMe)(3)]BF4 in Sulfuric Acid

ARTICLE *in* THE JOURNAL OF PHYSICAL CHEMISTRY A · AUGUST 2009

Impact Factor: 2.69 · DOI: 10.1021/jp903666p · Source: PubMed

6 AUTHORS, INCLUDING:

Begoña García
Universidad de Burgos
155 PUBLICATIONS **1,525** CITATIONS

SEE PROFILE

F. Javier Hoyuelos
Universidad de Burgos
18 PUBLICATIONS **121** CITATIONS

SEE PROFILE

Hydrolysis Mechanisms for the Organopalladium Complex $[Pd(CNN)P(OMe)_3]BF_4$ in Sulfuric Acid

Begoña García,* Francisco J. Hoyuelos, Saturnino Ibeas, María S. Muñoz, Indalecio Peñacoba, and José M. Leal

Departamento de Química, Universidad de Burgos, 09001 Burgos, Spain

Received: April 21, 2009; Revised Manuscript Received: May 27, 2009

The acid-catalyzed hydrolysis of the organopalladium complex $[Pd(CNN)P(OMe)_3]BF_4$ species was monitored spectrophotometrically at different sulfuric acid concentrations (3.9 and 11.0 M) in 10% v:v ethanol−water over the 25−45 °C temperature range and in 30% and 50% (v/v) ethanol−water at 25 °C. Two acidity regions (I and II) could be differentiated. In each of the two regions the kinetic data pairs yielded two different rate constants, k_{1obs} and k_{2obs}, the former being faster. These constants were fitted by an Excess Acidity analysis to different hydrolyses mechanisms: A-1, A-2, and A-S_E2. In region I ($[H_2SO_4] < 7.0$ M), the k_{1obs} values remained constant $k_{1obs}^{av} = 1.6 \times 10^{-3}$ s^{-1} and the set of k_{2obs} values nicely matched an A-S_E2 mechanism, yielding a rate-determining constant $k_{0,ASE2} = 2.4 \times 10^{-7}$ M^{-1} s^{-1}. In region II ($[H_2SO_4] > 7.0$ M), a switchover was observed from an A-1 mechanism ($k_{0,A1} = 1.3 \times 10^{-4}$ s^{-1}) to an A-2 mechanism ($k_{0,A2} = 3.6 \times 10^{-3}$ M^{-1} s^{-1}). The temperature effect on the rate constants in 10% (v/v) ethanol−water yielded positive $\Delta H^{\ddagger}$ and negative $\Delta S^{\ddagger}$ values, except for the A-1 mechanism, where $\Delta S^{\ddagger}$ adopted positive values throughout. The solvent permittivity effect, ε_r, revealed that k_{1obs}^{av} and $k_{0,A2}$ dropped with a fall in ε_r, whereas the $k_{0,ASE2}$ value remained unaffected. The set of results deduced is in line with the schemes put forward.

Introduction

Cyclometalation of organic substrates by transition metal complexes is an emerging field in organometallic chemistry and has been given increased attention.[1] Organic moieties may undergo metalation with formation of carbon−metal bonds by using transition metal complexes with two-electron donor atoms. Cyclometalated compounds constitute an important tool to activate the C−H σ bond stabilized by the additional coordination of the metal to a heterodonor atom, forming transition metal complexes. These structures have been suggested as frozen intermediate species in metal-catalyzed chemical reactions, thus contributing to shed light into the mechanism of such catalytic processes.[2] In most cases, the intramolecular activation of the C−H bond comes about with N-containing ligands, the metal quite often being palladium(II).[3] The chemistry of organopalladium complexes has developed increasingly over the last few decades; a number of reactions which had long been regarded as impracticable are now known to proceed smoothly with Pd catalysts, and several scientific dreams have become viable.[4] The cyclopalladated compounds formed this way quite often display a characteristic ability as starting materials in organic syntheses and have given way to a wide slate of reactions which proceed with notable regio- and stereoselectivity, leading to extensive possibilities for synthetic applications.[5]

However, despite the interest aroused by the chemistry of cyclopalladated compounds, so far only few kinetic and thermodynamic contributions have appeared, none of which were performed in highly acidic media.[6] In a previous paper, we reported the acid−base behavior of a set of four $[Pd(CNN)R]BF_4$ cyclopalladated complexes in concentrated sulfuric acid.[7] Likewise, the kinetics of the hydrolysis of 2-acetylpyridinephenylhydrazone (HCNN), a tricoordinated chelant donor ligand, was investigated in highly sulfuric acidic media.[8] With these precedents in mind, in this work we aim for a deeper knowledge on the pronounced stability of this type of organometallic complexes by looking into the hydrolyses of the title palladated complex in highly acidic media. Inasmuch as the reaction rate fell with rising solvent permittivity, the effect of aqueous−organic mixed solvents with different composition has also been undertaken using different ethanol−water mixtures.

Experimental Section

The $[Pd(CNN)P(OMe)_3]BF_4$ complex was synthesized as described elsewhere,[9] the other reagents being commercially available. The spectral curves were recorded on a computerized HP8452A spectrophotometer fitted out with a diode array detection system and a temperature cell-holder adapter. Inasmuch as the substrate is only sparingly soluble in pure water, the solvent effect on the kinetics was investigated using 10%, 30%, and 50% (v/v) ethanol−water solvents. Sulfuric acid was used to attain the required medium acidity in the 3.9−11.0 M range. The solutions used were prepared by careful addition of the appropriate H_2SO_4 amounts to 100 mL bottles containing known amounts of doubly distilled deionized water. For instance, substrate solutions in 30% (v/v) ethanol−water were freshly prepared directly in the quartz cell by syringing 0.30 mL of pure ethanol into 1.4 mL of the adequate H_2SO_4 solution; after the thermal equilibrium was reached, 0.30 mL of the proper substrate sample dissolved in pure ethanol (3.3×10^{-4} M) was added to the cell. A similar procedure was used with the other solvents.

The proton concentration, c_{H^+}, the Excess Acidity function *X*, defined as the extra acidity of the medium due to its nonideal behavior, and the water activities for each aqueous sulfuric acid concentration were all obtained from published sources.[10] Fulfillment of the Lambert−Beer law was assessed at all wavelengths used. Sets of acidity functions for sulfuric acid in ethanol−water mixtures are lacking in literature. However,

10.1021/jp903666p CCC: $40.75
Published on Web 07/21/2009

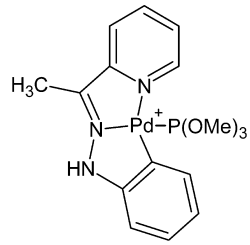

Figure 1. The palladium(II) complex $[Pd(CNN)P(OMe)_3]^+$ with the ligand 2-acetylpyridinephenylhydrazone (CNN).

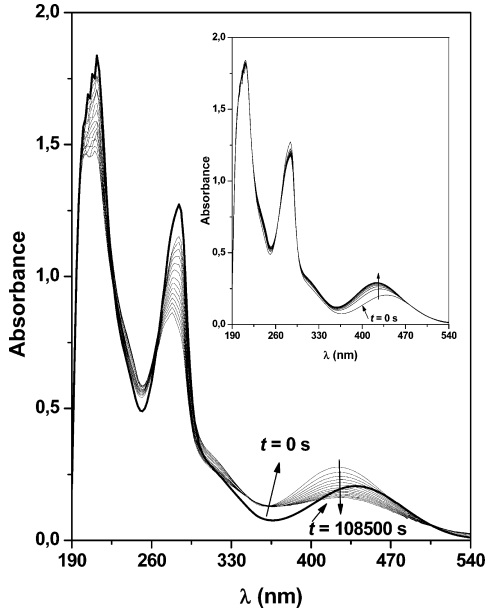

Figure 2. Absorption UV−vis spectral curves corresponding to hydrolysis of 5×10^{-5} M $[Pd(CNN)P(OMe)_3]^+$ complex in 10% (v/v) ethanol−water. $[H_2SO_4] = 5.2$ M, $T = 25$ °C; time interval between consecutive spectra, $\Delta t = 7750$ s. The insert shows the first step of consecutive reaction, $\Delta t = 155$ s.

considering that the ethanol effect on the pH measurements in 10% ethanol−water has been shown to be negligible,[11] a negligible effect on the excess acidity function can also be surmised. Hence, at 25 °C the X values introduced in 10% ethanol−water were those defined in aqueous solution, and for the other temperatures the X values were corrected according to[12]

$$X_T = \frac{298.15X_{25°C}}{(273.15 + T)} \quad (1)$$

In 30% and 50% ethanol−water the X values used were calculated from eq 2,[13] using the Hammett acidity function H_0, defined in these solvent media[14,15]

$$H_0 + \log c_{H^+} \approx -X \quad (2)$$

The kinetic data of two consecutive reactions can be analyzed by nonlinear least-squares fitting, using the double-exponential equation

$$A_t = \alpha e^{-k_{1obs}t} + \beta e^{-k_{2obs}t} + \gamma \quad (3)$$

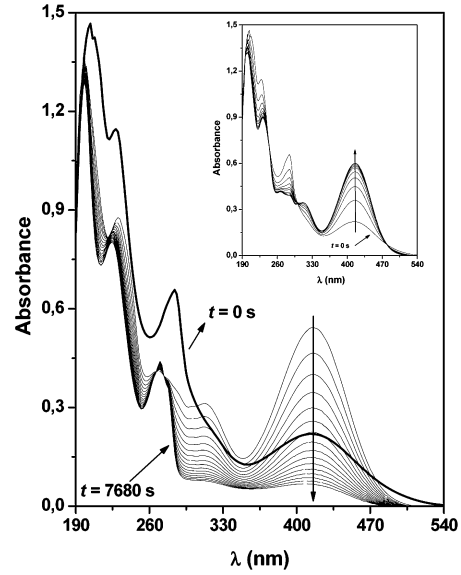

Figure 3. Absorption UV−vis spectral curves corresponding to hydrolysis of 5×10^{-5} M $[Pd(CNN)P(OMe)_3]^+$ complex in 10% (v/v) ethanol−water. $[H_2SO_4] = 9.1$ M, $T = 25$ °C; time interval between consecutive spectra, $\Delta t = 480$ s. The insert shows the first step of consecutive reaction, $\Delta t = 12$ s.

corresponding to the integrated rate equation for a reaction intermediate species, where A_t stands for the absorbance reading at time t at a given wavelength, α represents the rise in absorbance from the initial value to the maximum absorbance of the intermediate, β stands for the decline in absorbance from the maximum reached to completion, and γ is the absorbance at infinite time. The disappearance of the reactant was analyzed using the single-exponential equation

$$A_t = (A_0 - A_\infty)e^{-k_{1obs}t} + A_\infty \quad (4)$$

where A_0 and A_∞ stand for the initial and the final absorbance readings, respectively, and A_t represents that at intermediate time intervals.

To properly analyze the two processes independently from one another, the kinetic study was carried out by monitoring the decrease with time of the absorbances measured concurrently at the maximum wavelength and at the isosbestic points of the second process (365 and 274 nm in the lower and upper acidity region, respectively). Application of this procedure has enabled us to analyze in each acidity region the first kinetic process independently from the second, because at the isosbestic wavelengths the variation of the absorbance with time can be put down to solely the first process. The reactions were followed at least up to 90% completion, which corresponds to reaction times larger than 3.32 ln $2/k_{obs}$, k_{obs} being the observed rate constant.[16] The rate constants were independent of the substrate concentration in the acidity range investigated. Each rate constant was measured in triplicate, and the values concurred within 5%.

The nonlinear least-squares method has the advantage over Guggenheim's and similar methods[17] of requiring only a normal Gaussian error distribution of the fitting; the data pairs need not to be taken evenly, neither is it necessary to monitor the reaction to completion. The program used was based on the Marquardt−Levenberg algorithm;[18] after the initial estimated values are introduced, the process is iterated until the convergence is attained for the minimum value of the χ^2 parameter.

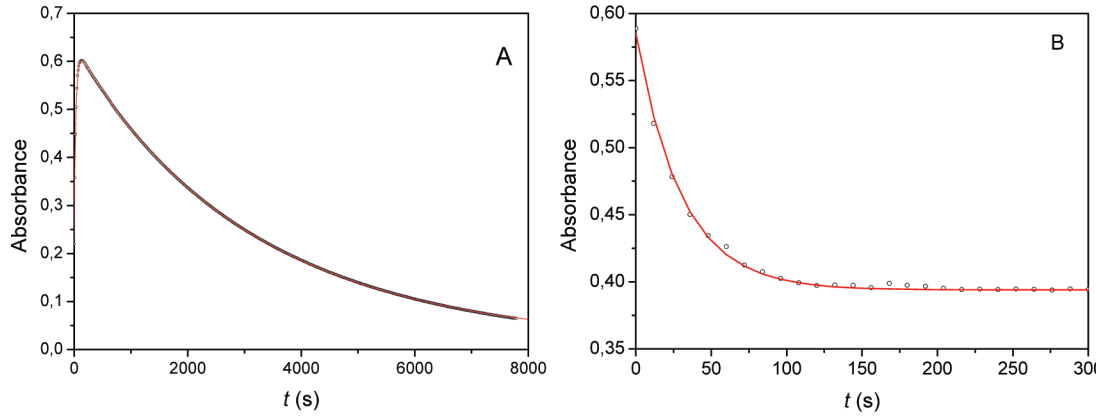

Figure 4. Absorbance vs time plots corresponding to the set of spectra of Figure 3: (A) $\lambda = 416$ nm, continuous line fitted with biexponential eq 3; (B) $\lambda = 274$ nm, continuous line fitted with monoexponential eq 4.

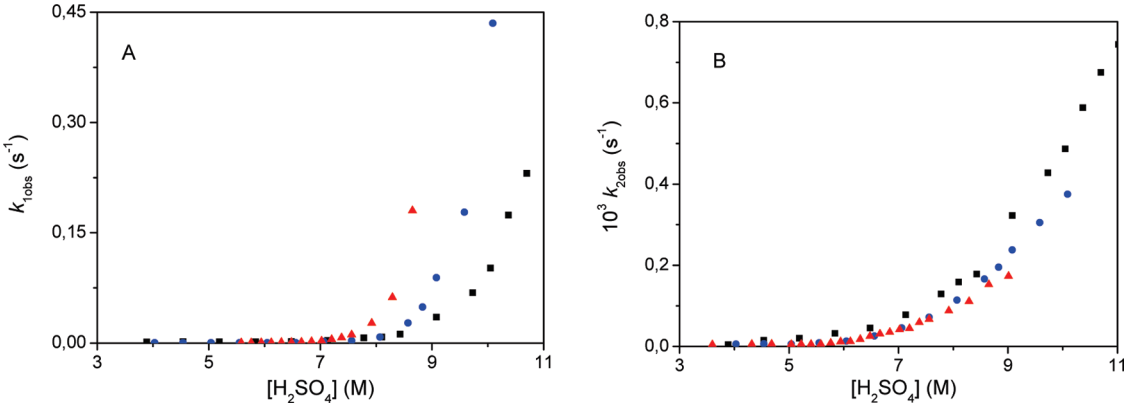

Figure 5. Plots of pseudo-first-order rate constants k_{1obs} (A) and k_{2obs} (B) vs molar sulfuric acid concentration for the hydrolysis of $[Pd(CNN)P(OMe)_3]^+$ at 25 °C: (□) 10% (v/v) ethanol−water; (●) 30% (v/v) ethanol−water; (▲) 50% (v/v) ethanol−water.

Kinetic Models

To determine the reaction mechanisms at medium and high acidity levels, outside the pH scale, a number of methods of dealing with kinetic data such as those of Zucker−Hammett,[19] Bunnett,[20] LFER,[21] and Cox−Yates[10,22] are available. The three first treatments establish the medium acidity in terms of the Hammett acidity function, H_0.[23] However, in this case the Excess Acidity method put forward by Cox−Yates was preferred insofar as it describes the system better. The excess acidity function, X, which displays the very useful feature of being zero in the standard state of activity coefficients unity, has become a powerful tool to study the medium acidity effect on equilibria and reaction rates, thus enabling us to distinguish between different hydrolysis mechanisms. Recently, a new set of measurements as a function of sulfuric acid concentration and temperature has come available.[24]

The Excess Acidity method has proved to be a valuable tool for the mechanistic elucidation of a wide variety of reactions in strongly acidic aqueous media, particularly in sulfuric acid. This treatment has been applied to the acid-catalyzed hydrolyses of lactams,[25] hydroxamic acids,[26,27] and antiinflammatory drugs,[28] including Wallach rearrangement of azoxypyridines.[29] Recently Cox has suggested a new mechanism for benzamide hydrolysis in strong acids[30] and reviewed the hydrolysis mechanisms of benzimidates, esters, and amides in aqueous sulfuric acid.[31] In acid media, reactions are most commonly catalyzed via mechanisms classified as A-1, A-2, or A-S_E2[32] as follows:

A-1 Mechanism. If, as occurs in this case, the starting material is $[Pd(CNN)P(OMe)_3]^+$, the unprotonated substrate (S^+), then the following mechanism applies

$$S^+ + H^+ \underset{\text{fast}}{\overset{K_{SH^{2+}}}{\rightleftharpoons}} SH^{2+} \quad (5)$$

$$SH^{2+} \xrightarrow[\text{slow}]{k_{0,A1}} A^{2+} \quad (6)$$

$$A^{2+} + H_2O \xrightarrow[\text{fast}]{} P \quad (7)$$

involving a fast protonation equilibrium of the substrate S^+, followed by the rate-determining unimolecular evolution of SH^{2+} either to an intermediate species A^{2+} (which subsequently reacts quickly) or directly to products. If, under the reaction conditions, the substrate is predominantly protonated, $c_{SH^{2+}} \gg c_{S^+}$, then the relevant rate equation is

$$\log k_{obs} - \log \frac{c_{SH^{2+}}}{c_{SH^{2+}} + c_{S^+}} = \log k_{0,A1} + (m^{\ddagger} - 1)m^*X \quad (8)$$

Publication Date (Web): July 21, 2009 | doi: 10.1021/jp903666p

TABLE 1: Rate Constants k_{1obs} and k_{2obs} in s^{-1} Calculated from Equations 3 and 4 for the Acid-Catalyzed Hydrolysis of $[Pd(CNN)P(OMe)_3]^+$ in Aqueous Sulfuric Acid at Different Temperatures and Acid Concentrations

10% (v/v) ethanol−water											
		25 °C		30 °C		35 °C		40 °C		45 °C	
$c_{H_2SO_4}$(M)	X[10]	$k_{1obs} \times 10^2$ (s^{-1})	$k_{2obs} \times 10^4$ (s^{-1})	$k_{1obs} \times 10^2$ (s^{-1})	$k_{2obs} \times 10^4$ (s^{-1})	$k_{1obs} \times 10^2$ (s^{-1})	$k_{2obs} \times 10^4$ (s^{-1})	$k_{1obs} \times 10^2$ (s^{-1})	$k_{2obs} \times 10^4$ (s^{-1})	$k_{1obs} \times 10^2$ (s^{-1})	$k_{2obs} \times 10^4$ (s^{-1})
3.89	1.097	0.137 ± 0.006	0.0464 ± 0.0008	0.232 ± 0.004	0.0934 ± 0.0005	0.309 ± 0.008	0.219 ± 0.002	0.457 ± 0.008	0.378 ± 0.002	0.603 ± 0.009	0.547 ± 0.003
4.54	1.335	0.176 ± 0.009	0.156 ± 0.002	0.321 ± 0.006	0.238 ± 0.002	0.454 ± 0.008	0.313 ± 0.003	0.672 ± 0.007	0.544 ± 0.003	0.839 ± 0.007	0.787 ± 0.003
5.19	1.582	0.158 ± 0.003	0.200 ± 0.001	0.294 ± 0.005	0.315 ± 0.001	0.389 ± 0.009	0.416 ± 0.002	0.664 ± 0.009	0.664 ± 0.003	0.884 ± 0.007	1.050 ± 0.003
5.84	1.836	0.152 ± 0.001	0.322 ± 0.002	0.251 ± 0.003	0.510 ± 0.003	0.342 ± 0.004	0.802 ± 0.003	0.515 ± 0.006	1.301 ± 0.003	0.652 ± 0.002	2.183 ± 0.006
6.48	2.091	0.198 ± 0.003	0.456 ± 0.002	0.298 ± 0.004	0.763 ± 0.003	0.416 ± 0.006	1.203 ± 0.004	0.613 ± 0.008	1.962 ± 0.007	0.936 ± 0.007	3.151 ± 0.006
7.13	2.355	0.330 ± 0.003	0.784 ± 0.002	0.448 ± 0.004	1.223 ± 0.003	0.629 ± 0.004	2.150 ± 0.005	0.946 ± 0.005	3.310 ± 0.005	1.285 ± 0.008	5.254 ± 0.009
7.78	2.627	0.711 ± 0.005	1.294 ± 0.003	1.020 ± 0.007	2.190 ± 0.005	1.31 ± 0.02	3.223 ± 0.006	2.42 ± 0.02	5.564 ± 0.008	2.83 ± 0.01	9.22 ± 0.01
8.10	2.764	0.827 ± 0.006	1.586 ± 0.003								
8.43	2.909	1.208 ± 0.007	1.783 ± 0.004	2.06 ± 0.01	3.059 ± 0.004	3.21 ± 0.02	4.976 ± 0.007	4.13 ± 0.01	8.166 ± 0.004	6.73 ± 0.02	12.90 ± 0.02
9.08	3.203	3.52 ± 0.01	3.223 ± 0.007	5.34[a] ± 0.09	5.253[a] ± 0.005	6.8[a] ± 0.2	8.194 ± 0.009	9.6[b] ± 0.1	13.29 ± 0.01	14.2[a] ± 0.3	21.42[a] ± 0.02
9.73	3.514	6.85 ± 0.09	4.28 ± 0.01	12.9[a] ± 0.3	7.50[a] ± 0.02	16.4[a] ± 0.2	11.84 ± 0.03	27.7[b] ± 0.5	20.33 ± 0.05	32[a] ± 2	31.42[a] ± 0.08
10.05	3.675	10.2 ± 0.2	4.87 ± 0.01								
10.37	3.840	17.4 ± 0.5	5.88 ± 0.02	*a*	10.07[a] ± 0.01	*a*	16.08 ± 0.03	*a*	24.48 ± 0.05	*a*	39.16[a] ± 0.07
10.70	4.016	23.1 ± 0.1	6.75 ± 0.02								
11.02	4.193	*a*	7.44 ± 0.02	*a*	12.52[a] ± 0.03	*a*	19.38 ± 0.05	*a*	30.52 ± 0.07	*a*	47.10[a] ± 0.09

30% (v/v) ethanol−water (T = 25 °C)			
$c_{H_2SO_4}$(M)	X[d]	$k_{1obs} \times 10^2$ (s^{-1})	$k_{2obs} \times 10^5$ (s^{-1})
4.03	1.248	0.060 ± 0.003	0.631 ± 0.007
4.54	1.509	0.058 ± 0.007	0.649 ± 0.007
5.04	1.779	0.040 ± 0.001	0.626 ± 0.002
5.55	2.068	0.043 ± 0.001	0.984 ± 0.007
6.05	2.362	0.059 ± 0.001	1.29 ± 0.01
6.56	2.672	0.062 ± 0.001	2.57 ± 0.02
7.06	2.985	0.219 ± 0.003	4.61 ± 0.02
7.56	3.307	0.322 ± 0.003	7.22 ± 0.01
8.07	3.643	0.813 ± 0.003	11.4 ± 0.2
8.57	3.979	2.75 ± 0.01	16.6 ± 0.2
8.83	4.157	4.89[a] ± 0.04	19.5[a] ± 0.2
9.08	4.323	8.89[a] ± 0.06	23.8[a] ± 0.3
9.58	4.680	17.8[a] ± 0.03	30.5[a] ± 0.5
10.09	1.248	43.5[a] ± 0.1	37.5[a] ± 0.1

50% (v/v) ethanol−water (T = 25 °C)			
$c_{H_2SO_4}$(M)	X[e]	$k_{1obs} \times 10^3$ (s^{-1})	$k_{2obs} \times 10^5$ (s^{-1})
3.60	1.867	*a*	0.471 ± 0.004
4.32	2.385	*a*, *c*	0.581 ± 0.007
4.68	2.649	*a*, *c*	0.588 ± 0.004
5.04	2.917	*a*, *c*	0.498 ± 0.004
5.22	3.051	*a*, *c*	0.575 ± 0.004
5.40	3.186	*a*, *c*	0.564 ± 0.004
5.58	3.322	0.47 ± 0.01	0.565 ± 0.004
5.76	3.459	0.65 ± 0.01	0.853 ± 0.002
5.94	3.595	0.80 ± 0.01	1.184 ± 0.004
6.12	3.733	0.86 ± 0.01	1.219 ± 0.003
6.30	3.871	0.93 ± 0.01	1.760 ± 0.002
6.48	4.009	1.00 ± 0.01	2.540 ± 0.009
6.66	4.147	1.44 ± 0.01	3.091 ± 0.008
6.84	4.286	2.08 ± 0.02	3.492 ± 0.008
7.02	4.426	2.99 ± 0.04	4.18 ± 0.01
7.20	4.565	4.93 ± 0.09	4.45 ± 0.01
7.38	4.706	7.49 ± 0.04	5.93 ± 0.01
7.56	4.846	11.24 ± 0.03	6.69 ± 0.02
7.92	5.128	27.01 ± 0.09	8.78 ± 0.01
8.29	5.418	62.2 ± 0.5	11.10 ± 0.01
8.65	5.702	180 ± 5	15.27 ± 0.05
9.01	5.987	[d]	17.31[a] ± 0.06

[a] The first process is fast and could not be measured. [b] Because the second process is very slow, it cannot record enough data for the first process. [c] Using eq 2. H_0 from ref 13.

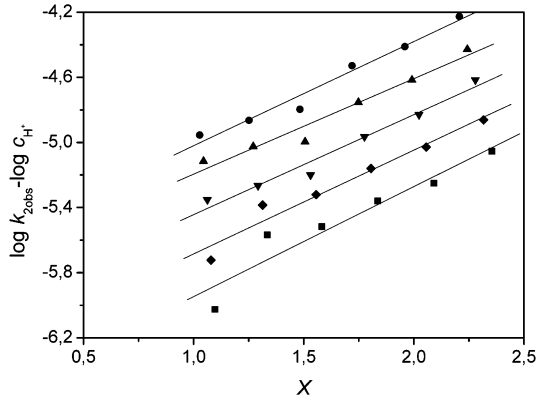

Figure 6. log k_{2obs} − log c_{H^+} vs X (sulfuric acid) plot corresponding to an A-S_E2 mechanism, eq 16, 10% (v/v) ethanol−water, at different temperatures: (□) 25 °C, (◆) 30 °C, (▼) 35 °C, (▲) 40 °C, and (●) 45 °C.

The slope parameter $m^{\ddagger}$ accounts for the location of the transition state and correlates the substrate activity coefficients with those of the transition state according to

$$\log \frac{f_{S^+} f_{H^+}}{f_{\ddagger}} = m^{\ddagger} \log \frac{f_{S^+} f_{H^+}}{f_{SH^{2+}}} = m^{\ddagger} m^* X \qquad (9)$$

The m^* parameter, defined in eq 10, relates the substrate activity coefficients to those of the standard base that serves to define the X function and reflects the susceptibility of the protonated substrate to become stabilized by solvation

$$\log \frac{f_{S^+} f_{H^+}}{f_{SH^{2+}}} = \log \frac{f_B f_{H^+}}{f_{BH^+}} = m^* X \qquad (10)$$

To find out the $m^{\ddagger}$ value and therefore to be able to establish the reaction mechanism, the proper m^* value corresponding to the protonation equilibrium in high acidity media, $pK_{SH^{2+}}$, must be evaluated. The m^* values are temperature independent.[10,33] The plot of the left-hand side of eq 8 vs X should yield a straight line, whose ordinate provides the log $k_{0,A1}$ value. In addition, the $m^{\ddagger}$ value should be greater than 1.[34,35]

A-2 Mechanism. This is similar to A-1 except that the protonated substrate, SH^{2+}, instead of evolving alone, reacts with another species in the bimolecular rate-determining step

$$S^+ + H^+ \underset{\text{fast}}{\overset{K_{SH^{2+}}}{\rightleftharpoons}} SH^{2+} \qquad (11)$$

$$SH^{2+} + n\text{Nu} \xrightarrow[\text{slow}]{k_{0,A2}} P \qquad (12)$$

where Nu stands for the nucleophile, normally water, and n is the number of molecules. The corresponding derived Excess Acidity rate equation, which governs the hydrolysis for predominantly unprotonated substrates, has the form

$$\log k_{obs} - \log \frac{c_{S^+}}{c_{SH^{2+}} + c_{S^+}} - \log c_{H^+} - n \log a_{Nu} = \log \frac{k_{0,A2}}{K_{SH^{2+}}} + m^{\ddagger} m^* X \qquad (13)$$

where the parameter $m^{\ddagger}$ must be close to unity[34,36] and the protonation correction term $\log(c_{S^+}/(c_{SH^{2+}} + c_{S^+}))$ reflects the feature that the substrate is not fully protonated at higher acid concentrations.[22] To be able to plot the left-hand side of eq 13 vs X, the $k_{0,A2}$ parameter can be determined if the equilibrium constant is previously known.

A-S_E2 Mechanism. The bimolecular pathway put forward by Cox involves a rate-determining proton transfer to the monoprotonated substrate:[22]

$$S^+ + H^+ \underset{\text{slow}}{\overset{k_{0,ASE2}}{\rightleftharpoons}} SH^{2+} \qquad (14)$$

$$SH^{2+} + H_2O \xrightarrow[\text{fast}]{} P \qquad (15)$$

that yields the rate equation

$$\log k_{obs} - \log c_{H^+} = \log k_{0,ASE2} + m^{\ddagger} m^* X \qquad (16)$$

The plot of the left-hand side of eq 16 vs X has enabled us to determine the $k_{0,ASE}$ value. For an A-S_E2 scheme the $m^{\ddagger}$ value, characteristic of the type of mechanism, should be less than 1.[37]

Results and Discussion

The kinetic data will then be discussed in terms of the Excess Acidity analyses and potential mechanistic switchover. The acid hydrolysis of the $[Pd(CNN)P(OMe)_3]BF_4$ complex (Figure 1) was studied in highly acidic 10% (v/v) ethanol−water mixtures over the 25−45 °C temperature range. In 30% and 50% (v/v) ethanol−water the working temperature was 25 °C. Figures 2 and 3 show the UV−vis spectral curves recorded at different time intervals in 5.2 and 9.1 M sulfuric acid, respectively; in both cases two consecutive pseudo-first-order reactions could be differentiated. The two sets of spectral curves clearly differed in shape, which points up that different active species are involved depending on the medium acidity. Figure 4 shows the biexponential absorbance decay of the spectral curves recorded in the region of the intermediate species (416 nm) and the monoexponential decay observed for the substrate at 274 nm, where the spectral curves of the second step display an isosbestic point. The k_{obs} rate constants at 416 nm were deduced from the nonlinear least-squares fitting using eq 3 and the absorbance values for the disappearance of the reactant, 274 nm, were analyzed using eq 4. The values deduced for k_{1obs} with eq 4 matched fairly well with those arising from eq 3. Table 1 lists the values deduced for the observed k_{1obs} and k_{2obs} rate constants as a function of acidity, temperature, and ethanol−water content. The k_{1obs} constants were larger than k_{2obs} across the whole acidity range. Figure 5 shows the change of k_{1obs} and k_{2obs} with the H_2SO_4 concentration using mixed solvents of different composition.

Hydrolysis Mechanisms. The kinetic criteria established to discriminate between different hydrolysis mechanisms were applied to the sets of data pairs. To this aim, the overall acidity range outlined in Figure 5 was split into two well-differentiated stretches. In region I (3.6−6.5 M sulfuric acid) the hydrolysis rate constants increased only very smoothly with rising acidity. By contrast, in region II (6.5−11.0 M sulfuric acid) the rates increased sharply without hinting at a plateau even at fairly high

TABLE 2: Rate-Determining Constants ($k_{0,A}$), and $m^{\ddagger}$ Values at Several Temperatures, for $[Pd(CNN)P(OMe)_3]^+$ Reacting via the Three Mechanisms in Sulfuric Acid

	10% v:v ethanol−water					30% v:v ethanol−water	50% v:v ethanol−water
	25 °C	30 °C	35 °C	40 °C	45 °C	25 °C	25 °C
				Low Acidity Region (3.6−6.5 M H_2SO_4)			
k_{1obs}^{av}	1.92×10^{-3}	3.07×10^{-3}	4.23×10^{-3}	6.45×10^{-3}	8.67×10^{-3}	5.37×10^{-4}	5.60×10^{-4}
				A-S_E2 mechanism (eq *16*)			
$k_{0,ASE2}$ (M^{-1} s^{-1})	2.39×10^{-7}	4.76×10^{-7}	8.75×10^{-7}	1.66×10^{-6}	2.20×10^{-6}	1.21×10^{-7}	2.98×10^{-7}
$m^{\ddagger}$	0.61	0.58	0.56	0.53	0.58	0.57	0.50
				High Acidity Region (6.5−11.0 M H_2SO_4)			
				A-1 mechanism (eq *8*)			
$k_{0,A1}$ (s^{-1})	1.25×10^{-4}	3.06×10^{-4}	6.59×10^{-4}	1.47×10^{-3}	2.89×10^{-3}	9.29×10^{-2}	2.21×10^{-3}
$m^{\ddagger}$	1.74	1.70	1.66	1.63	1.59	1.60	1.52
				A-2 mechanism (eq *13*)			
$k_{0,A2}$ (M^{-1} s^{-1})	3.56×10^{-3}	5.38×10^{-3}	9.58×10^{-3}	1.68×10^{-2}	2.90×10^{-2}	1.59×10^{-3}	8.40×10^{-4}
$m^{\ddagger}$	1.04	1.07	1.07	1.07	1.08	0.78	0.83

SCHEME 1: Mechanism for the Hydrolysis of $[Pd(CNN)(OMe)_3]^+$ in the 3.6−6.5 M H_2SO_4 Acidity Region

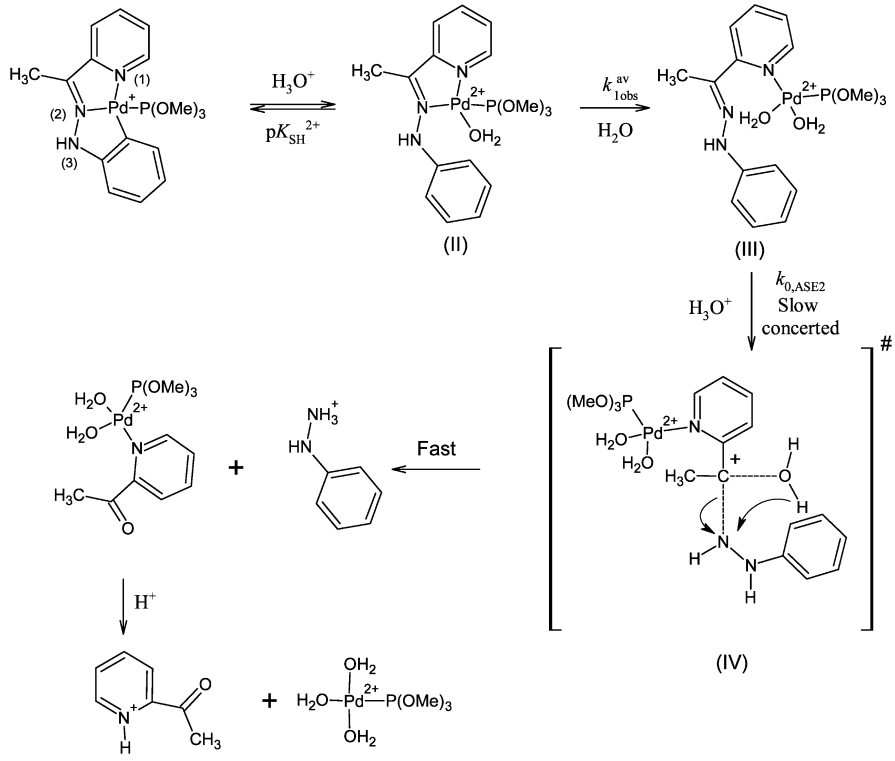

acidities, which suggests that the two regions are governed by different mechanisms.

Region I. In this acidity range two consecutive pseudo-first-order reactions were observed (Figures 2 and 5). The faster reaction, k_{1obs}, is unaffected by the change in the medium acidity (Table 1 and Figure 5A). For the slower process, k_{2obs}, the rate constants varied with medium acidity only smoothly (Figure 5 B) and were scrutinized in light of eqs 8, 13, and 16. The A-S_E2 mechanism, eq 16, best fitted the kinetic constants (Figure 6). The $m^{\ddagger} = 0.57$ value deduced for the different temperatures and ethanol contents concurs with the Cox−Yates criterion established for the A-S_E2 mechanism (Table 2). The $k_{0,ASE2}$ rate constants deduced for the rate-determining step at several temperatures are given in Table 2. To our knowledge, no upper limit for the $k_{0,ASE2}$ value has in principle been reported in literature for the wide variety of reactions that follow the A-S_E2 mechanism.[22,38−40]

The mechanism put forward is outlined in Scheme 1. In a previous work, we calculated the dissociation constant $pK_{SH^{2+}} = -4.2$ for the $[Pd(CNN)P(OMe)_3]BF_4$ complex protonated in the orthopalladated C atom (form II).[4] In this acidity region the k_{1obs} values were essentially independent of the proton concentration (Table 1, below 6.5 M H_2SO_4). In the presence of a solvent, the complex undergoes an addition reaction by an incoming ligand over its square-planar Pd atom (form III), the averaged rate constant being $k_{1obs}^{av} = 1.6 \times 10^{-3}$ s^{-1}. The potent σ donor nature of the $P(OMe)_3$ moiety renders the Pd−$P(OMe)_3$ bonding stronger, and the Pd-*trans* N bonding weaker, the latter becoming broken.[6] Hence, the k_{1obs}^{av} rate constant accounts for the rupture of the N−Pd bond.

Therefore, both water and ethanol can in principle be regarded as suitable candidates as incoming ligands. Hardness/softness relationships and steric considerations can be of help to scrutinize which of the two candidates may act as a reactant species. Using heats of formation, proton affinities, and ionization potential data, Pearson has shown that CH_3OH is 1.4 times harder than H_2O.[41] In view of the lack of hardness data for ethanol, a value for ethanol closer to methanol than to water

SCHEME 2: Mechanism for the Hydrolysis of $[Pd(CNN)P(OMe)_3]^+$ in the 7.0−11.0 M H_2SO_4 Acidity Region

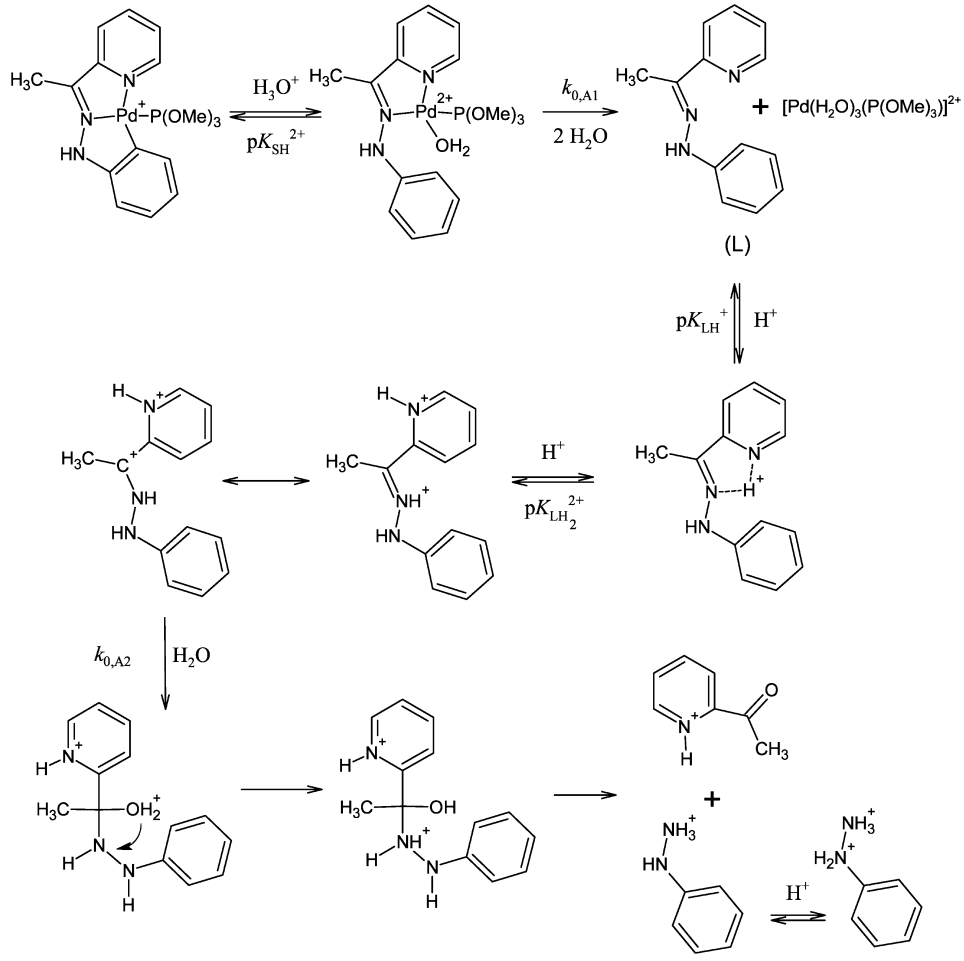

can be surmised; this feature and the weaker water steric effect have enabled us to suggest water as the preferred ligand (form III). Finally, the $P(OMe)_3$ ligand promotes a strong trans effect. The pronounced tendency of this kind of compound to hold the equatorial position in the reaction intermediate forces the ligand in a trans position with regard to $P(OMe)_3$ to hold the same position.

The data analysis for the second process, k_{2obs}, is consistent with an A-S_E2 mechanism; Figure 6 shows the good fitting of eq 16 to the kinetic data collected at different temperatures. The mechanism commences with the attack of a second proton to the $N_{(2)}$ atom in the hydrazone of form III. Such an attack is more difficult for syn conformers; thus the rotation of the C−H σ bond is feasible and gives rise to an anti conformation transition state. The data analysis is consistent with an A-S_E2 mechanism with a trication species as the transition state, bearing two positive charges on the Pd atom and the third one on the C atom. Whereas the C−N bond becomes more labile, a water molecule stabilizes the transition state by a concerted mechanism. The rate-determining step is the formation of the activated

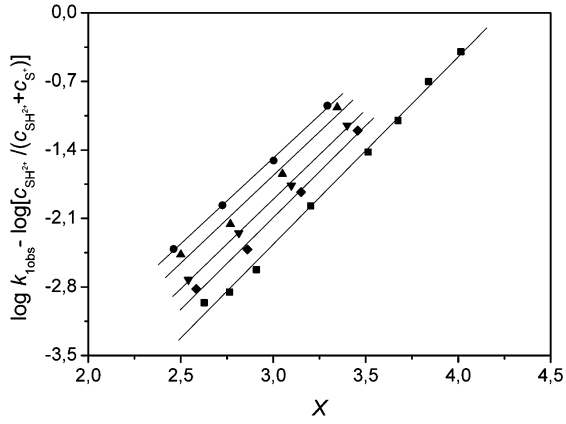

Figure 7. $\log k_{1obs} - \log(c_{SH^{2+}}/(c_{SH^{2+}} + c_{S^+})$ vs X (sulfuric acid) plot for an A-1 mechanism, eq 8, 10% (v/v) ethanol−water, at different temperatures: (□) 25 °C, (◆) 30 °C, (▼) 35 °C, (▲) 40 °C, and (●) 45 °C.

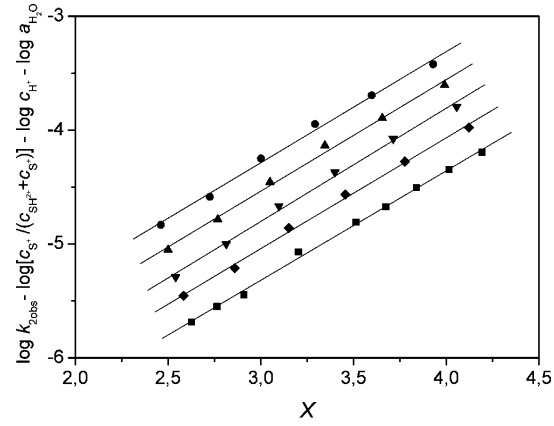

Figure 8. $\log k_{2obs} - \log(c_{S^+})/(c_{SH^{2+}} + c_{S^+}) - \log c_{H^+} - \log a_{H_2O}$ vs X (sulfuric acid) plot for an A-2 mechanism, eq 13, 10% (v/v) ethanol−water, at different temperatures: (□) 25 °C, (◆) 30 °C, (▼) 35 °C, (▲) 40 °C, and (●) 45 °C.

TABLE 3: Activation Parameters Obtained from the Rate Constants of the Rate-Determining Step in 10% (v/v) Ethanol−Water

	$\Delta H^{\ddagger}$/kJ mol^{-1}	$\Delta S^{\ddagger}$/J K^{-1} mol^{-1}	r	eqs
k_{1obs}^{av}	57 ± 2	−106 ± 7	0.998	*17*
	59 ± 2	−98 ± 7	0.998	*18*
$k_{0,ASE2}$	87 ± 6	−78 ± 19	0.993	*17*
	90 ± 6	−70 ± 19	0.994	*18*
$k_{0,A1}$	122 ± 2	88 ± 7	0.999	*17*
	124 ± 2	96 ± 7	0.999	*18*
$k_{0,A2}$	81 ± 3	−19 ± 11	0.998	*17*
	84 ± 3	−11 ± 10	0.998	*18*

complex, followed by a fast step that evolves to reaction products (Scheme 1). Phenylhydrazine possesses two different basic sites prone to protonation p$K_1 = 7.95$[42] and p$K_2 = -5.2$[43] (H_0 value for half-protonation). Theoretical calculations have demonstrated that it is the nonsubstituted N atom that becomes preferentially protonated.[44] Brignell et al.[42] reported ten H_0 units separation between the first and the second protonation in substituted phenylhydrazines.[45] In this acidity region only the monoprotonated phenylhydrazine form is present.

Region II. Like in region I, the mechanism in region II (between 7.0 and 11.0 M H_2SO_4) consists of two consecutive reactions with rate constants k_{1obs} and k_{2obs} (Scheme 2). The kinetic data of the first effect, k_{1obs}, nicely fulfilled eq 8 at all temperatures (Figure 7) and yielded an averaged $m^{\ddagger} = 1.7$ value (Table 2), concurrent with the Cox−Yates requirement for an A-1 mechanism. Comparison of the spectral curves corresponding to the second process (Figure 3) with those corresponding to the hydrolysis of the 2-acetylpyridinephenylhydrazone (L) ligand indicates that the two sets of curves match the same species and that L is an intermediate species of the $[Pd(CNN)P(OMe)_3]BF_4$ hydrolysis. In fact, two acidity dissociation constants were reported earlier[8] for the L ligand, pK_{LH^+}= 5.2 and p$K_{LH_2^{2+}} = -5.8$. The fitting of eq 13 to the k_{2obs} values deduced at all temperatures (Figure 8) using p$K_{LH_2^{2+}} = -5.8$, and $m^* = 0.94$,[8] yielded the averaged value $m^{\ddagger} = 1$ (Table 2), which concurs with the A-2 mechanism, $n = 1$ being the number of water molecules involved in the bimolecular mechanism. To evaluate the $m^{\ddagger}$, m^*, and log $k_{0,A2}$ parameters for the A-2 mechanism in 30% and 50% ethanol−water, nonlinear least-squares minimization iterations according to eq 13 were also carried out (Table 2). On the basis of the dissociation constant obtained (p$K_2 = -5.2$) phenylhydrazine is partially diprotonated in this acidity region.[41]

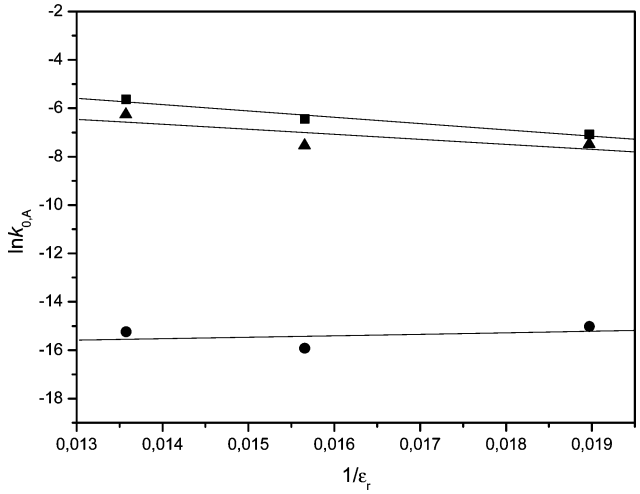

Figure 9. Variation of ln $k_{0,A}$ vs $1/\varepsilon_r$. $T = 25$ °C: (▲) ($k_{0,A} = k_{1obs}^{av}$); (■) A-2 mechanism ($k_{0,A} = k_{0,A2}$); (●) A-S$_E$2 mechanism ($k_{0,A} = k_{0,ASE2}$).

Temperature Effect. Reaction rates almost always increase with temperature.[15] Two forms are commonly used to express the temperature effect on the rate constants, the Arrhenius equation and the transition state theory Eyring equation[46]

$$\ln \frac{k_{0,A}h}{kT} = \frac{\Delta S^{\ddagger}}{R} - \frac{\Delta H^{\ddagger}}{RT} \qquad (17)$$

where $k_{0,A}$ is the rate constant, h, k, and R are universal constants, and $\Delta S^{\ddagger}$ and $\Delta H^{\ddagger}$ are the entropy and the enthalpy of activation, respectively. According the Absolute Rate Theory and using the Clarke and Glew method[47] (Cox[30,31] found it advantageous over the usual Eyring expansion) to express log $k_{0,i}$ in terms of $\Delta G^{\ddagger}$ and $\Delta H^{\ddagger}$

$$\log k_{0,A} = 10.31883 + \log T - \left(\frac{\Delta G^{\ddagger}}{RT \ln 10}\right) + \left(\frac{\Delta H^{\ddagger}}{RT \ln 10}\right)\left(\frac{T-\theta}{T}\right) \qquad (18)$$

where $\Delta G^{\ddagger}$ is the activation free energy; the activation entropy $\Delta S^{\ddagger}$ can easily be obtained from $\Delta G^{\ddagger} = \Delta H^{\ddagger} - T\Delta S^{\ddagger}$. All the activation parameters were obtained at the reference temperature, $\theta = 298.15$ K. The activation parameters obtained using eqs 17 and 18 from the log $k_{0,A}/T$ vs $1/T$ plots are very similar (Table 3).

The activation entropy, related to the reaction probability, includes orientational, steric, bulk, and solvation contributions. If, nevertheless, the activation process involves dissociation effects such as bond breaking within the single species, then a large and positive $\Delta S^{\ddagger}$ value is likely. As stated earlier, the $\Delta S^{\ddagger}$ value for a bimolecular reaction relies on the choice of the concentration scale. For rate constants in dm^3 mol^{-1} s^{-1} units, the $\Delta S^{\ddagger}$ value is likely to be substantially negative, at least if the second-order kinetics is a manifestation of a bimolecular mechanism, not a more complicated scheme.[16] The vast majority of substitution reactions in square-planar complexes undergo an associative mechanism reflected by the negative $\Delta S^{\ddagger}$ value.[48] The negative activation entropies for the A-S$_E$2 and A-2 mechanisms bear out a bimolecular reaction, whereas the positive $\Delta S^{\ddagger}$ value for the A-1 scheme indicates, as suggested, a unimolecular process. The $\Delta S^{\ddagger}$ values deduced (Table 3) also show that in region I the first reaction, k_{1obs}^{av}, undergoes an associative mechanism, confirming the proposed scheme.

Solvent Effect. In this study, 10, 30, and 50% (v/v) ethanol−water mixed solvents were used, with solvent permittivity values, 73.67, 63.88, and 52.72, respectively.[49] The rate-determining constants k_0 are independent of the medium acidity. Several formulations have been developed to interpret the solvent permittivity effect for ion−ion, ion−dipole, and dipole−dipole reactions in solution. For the ion−ion reaction, A-S$_E$2 mechanism (Scheme 1), the ln $k_{0,ASE2}$ vs $1/\varepsilon_r$ dependence fulfills eq 19[16]

$$\ln k_{0,ASE2} = \ln k_{ref} - \frac{NZ_AZ_Be^2}{(4\pi\varepsilon_o)\varepsilon_r RTr_{\ddagger}} \qquad (19)$$

where k_{ref} is the rate constant in the reference state of a hypothetical solvent of infinite dielectric permittivity. In this

work, the slope of the straight line should be negative, consistent with the obvious feature that the transition state is more polar than the positively charged reagents; however, Figure 9 shows that the slope is close to 0, concurrent with the concerted mechanism put forward (Scheme 1). For ion−dipole interactions, constant k_{1obs}^{av} values, and the A-2 mechanism (Schemes 1 and 2), the following formulation was developed for the limit case of a zero approximation ion−dipole angle

$$\ln k_0 = \ln k_{ref} - \frac{NZ_e^2}{(4\pi\varepsilon_o)2\varepsilon_r RT}\left(\frac{1}{r_{ion}} - \frac{1}{r_{\ddagger}}\right) \qquad (20)$$

where k_0 stands for k_{1obs}^{av} and $k_{0,A2}$.

The slope of the $\ln k_0$ vs $1/\varepsilon_r$ plot depends on the relative r_{ion} and $r_{\ddagger}$ values, the ion and transition state radii. The negative slope (Figure 9) reveals that r_{ion} is smaller than $r_{\ddagger}$, consistent with the proposed mechanisms.

Acknowledgment. The financial support by Ministerio de Educación y Ciencia, Project CTQ2006-14734/BQU, supported by FEDER, and Junta de Castilla y León, Project BU 013A09, Spain, is gratefully acknowledged.

References and Notes

(1) Dunina, V. V.; Zalevskaya, O. A.; Potapov, V. M. *Russ. Chem. Rev.* **1988**, *57*, 250.
(2) Crabtree, R. H. *Chem. Rev.* **1985**, *85*, 245.
(3) Dupont, J.; Beydoun, N.; Pfeffer, M. *J. Chem. Soc., Dalton Trans.* **1989**, 1715.
(4) Tsuji, J. *Palladium Reagents and Catalysts. New Perspectives for the 21st Century*; Wiley: London, 2004.
(5) Ryabov, A. D. *Synthesis* **1985**, 233.
(6) Crabtree, R. H. *The Organometallic Chemistry of the Transition Metals*, 4th ed.; Wiley: New York, 2005; p 6.
(7) Muñoz, M. S.; García, B.; Ibeas, S.; Hoyuelos, F. J.; Peñacoba, I.; Navarro, A. M.; Leal, J. M. *New J. Chem.* **2004**, *28*, 1450.
(8) García, B.; Muñoz, M. S.; Ibeas, S.; Leal, J. M. *J. Org. Chem.* **2000**, *65*, 3781.
(9) García-Herbosa, G.; Muñoz, A.; Miguel, D.; García-Granda, S. *Organometallics* **1994**, *13*, 1775.
(10) Cox, R. A. *Adv. Phys. Org. Chem.* **2000**, *35*, 1.
(11) Bates, R. G. *Determination of pH. Theory and practice*; Wiley: New York, 1973; p 244.
(12) Cox, R. A.; Goldman, M. F.; Yates, K. *Can. J. Chem.* **1979**, *57*, 2960.
(13) (a) Lucchini, V.; Modena, G.; Scorrano, G.; Cox, R. A.; Yates, K. *J. Am. Chem. Soc.* **1982**, *104*, 1958–1959. (b) Perdoncin, G.; Scorrano, G. *J. Am. Chem. Soc.* **1977**, *99*, 6983–6986.
(14) Dolman, D.; Stewart, R. *Can. J. Chem.* **1967**, *45*, 903.
(15) White, W. N.; Vogelmann, T.; Morse, M.; White, H. S. *J. Org. Chem.* **1977**, *42*, 162.
(16) Espenson, J. H. *Chemical Kinetics and Reaction Mechanisms*, 2nd ed.; McGraw-Hill: New York, 1995, chs 2, 9.
(17) Moore, P. *J. Chem. Soc., Faraday Trans. 1* **1972**, *68*, 1890.
(18) Cai, Q. Y.; Wang, R. G.; Wu, L. Y.; Nie, L. H.; Yao, S. Z. *Talanta* **1996**, *43*, 699.
(19) Zucker, L.; Hammett, L. P. *J. Am. Chem. Soc.* **1939**, *61*, 2791.
(20) Bunnett, J. F. *J. Am. Chem. Soc.* **1961**, *83*, 4956.
(21) Bunnett, J. F.; Olsen, F. P *Chem. Commun.* **1965**, 601. Bunnett, J. F.; Olsen, F. P *Can. J. Chem.* **1966**, *44*, 1899.
(22) Cox, R. A. *Acc. Chem. Res.* **1987**, *20*, 27.
(23) Hammett, L. P.; Deyrup, A. J. *J. Am. Chem. Soc.* **1932**, *54*, 2721.
(24) Myhre, C. E. L.; Christensen, D. H.; Nicolaisen, F. M.; Nielsen, C. J. *J. Phys. Chem. A* **2003**, *107*, 1979.
(25) Cox, R. A. *Can. J. Chem.* **1998**, *76*, 649.
(26) García, B.; Ibeas, S.; Hoyuelos, F. J.; Leal, J. M.; Secco, F.; Venturini, M. *J. Org. Chem.* **2001**, *66*, 7986.
(27) Ghosh, K. K.; Vaidya, J.; Sinha, D. *Z. Phys. Chem.* **2004**, *218*, 563.
(28) García, B.; Hoyuelos, F. J.; Ibeas, S.; Leal, J. M. *J. Org. Chem.* **2006**, *71*, 3718.
(29) Buncel, E.; Keum, S. R.; Rajagopal, S.; Kiepek, E.; Cox, R. A. *Can. J. Chem.* **2008**, *86*, 298.
(30) Cox, R. A. *Can. J. Chem.* **2008**, *86*, 290.
(31) Cox, R. A. *Can. J. Chem.* **2005**, *83*, 1391.
(32) Cox, R. A.; Yates, K. *Can. J. Chem.* **1981**, *59*, 1560.
(33) Bentley, T. W. *Can. J. Chem.* **2008**, *86*, 277.
(34) Cox, R. A.; Yates, K. *Can. J. Chem.* **1979**, *57*, 2944.
(35) Lajunen, M.; Uotila, R. *Acta Chem. Scand.* **1992**, *46*, 968.
(36) Cox, R. A.; Smith, C. R.; Yates, K. *Can. J. Chem.* **1979**, *57*, 2952.
(37) Cox, R. A.; Yates, K. *J. Am. Chem. Soc.* **1978**, *100*, 3861.
(38) Churchill, D.; Dust, J. M.; Buncel, E. *Can. J. Chem.* **2007**, *85*, 421.
(39) Cox, R. A.; McAllister, M.; Roberts, K. A.; Stang, P. J.; Tidwell, T. T. *J. Org. Chem.* **1989**, *54*, 4899.
(40) (a) Ali, M.; Satchell, D. P. N. *J. Chem. Soc., Perkin Trans. 2* **1992**, 219. (b) Joseph, V. B.; Satchell, D. P. N.; Satchell, R. S.; Wassef, W. N. *J. Chem. Soc., Perkin Trans. 2* **1992**, 339. (c) Ali, M.; Satchell, D. P.N.; Le, V. T. *J. Chem. Soc., Perkin Trans. 2* **1993**, 917. (d) Cox, R. A *J. Phys. Org. Chem.* **1991**, *4*, 233.
(41) Pearson, R. G. *J. Am. Chem. Soc.* **1988**, *110*, 7684.
(42) Stewart, R. *The Proton: Applications to Organic Chemistry*; Academic Press, Inc.: New York, 1985; p 199.
(43) Brignell, P. J.; Johnson, C. D.; Katritzky, A. R.; Shakir, N.; Tarhan, H. O.; Walker, G. *J. Chem. Soc. B* **1967**, 1233.
(44) Bagno, A.; Menna, E.; Mezzina, E.; Scorrano, G.; Spinelli, D. *J. Phys. Chem. A* **1998**, *102*, 2888.
(45) Cox, R. A.; Yates, K. *Can. J. Chem.* **1984**, *62*, 1613.
(46) Wynne-Jones, W. F. K.; Eyring, H. *J. Chem. Phys.* **1935**, *3*, 492.
(47) Clarke, E. C. W.; Glew, D. N. *Trans. Faraday Soc.* **1966**, *62*, 539.
(48) Wilkins, R. G. *Kinetics and Mechanism of Reactions of Transition Metal Complexes*, 2nd ed.; VCH: New York, 1991; p 235.
(49) Funasaki, N.; Hada, S.; Neya, S. *J. Phys. Chem.* **1985**, *89*, 3046.

JP903666P